45

63-2-2

AD No. 294661

ASTIA FILE COPY

1

NP-12144

Report Number

294 661

$ 4.60

ASTIA
RECEIVED
JAN 24 1963
TISIA

United States Atomic Energy Commission

Division of Technical Information

OTI-131(May 1962)

USAEC Division of Technical Information Extension, Oak Ridge, Tennessee

NP-12144

INVESTIGATION OF THE PHYSICAL METALLURGY OF JOINING TUNGSTEN AND COLUMBIUM

Quarterly Progress Report No. 6

(DM62-217)

Contract No. AF33(616)-7484

August 31, 1962

Flight Propulsion Laboratory Department
General Electric Company
Cincinnati 15, Ohio

TABLE OF CONTENTS

FOREWORD

This is the sixth quarterly report by the Flight Propulsion Laboratory Department of the General Electric Company under USAF - Aeronautical Systems Division - Contract No. AF33(616)-7484, with Mr. R. E. Bowman serving as Project Engineer.

The work is being done in the Materials and Processes Sub-Operation laboratory, Applied Research Operation. General Electric personnel responsible for the conduct of the work are:

Part I	-	Brazing Alloy Systems For Columbium And Tungsten - W. R. Young
Part II	-	Tungsten Alloy Ductility Improvement - J. W. Clark
Part III	-	Diffusion Bonding Studies was completed by the late E. S. Jones.

Approval: W H Chang

W. H. Chang - Acting Project Manager
Materials and Processes - ARO
Flight Propulsion Laboratory Dept.
General Electric Company
Cincinnati 15, Ohio

SUMMARY

This summarizes progress during the sixth quarterly reporting period

Part I - Brazing Alloy Systems For Columbium And Tungsten

The metallographic analysis of ~~fourteen~~ 14 new braze alloys for ~~columbium~~ niobium was completed ~~and summary data sheets for each alloy were prepared~~. Braze alloys selected for strength evaluation were: AS-540 (60V-30Cb-10Ti), AS-541 (60V-30Cb-10Ti-.2C), AS-546 (60V-30Cb-10Zr), AS-547 (59V-29Cb-10Zr-2Si), and AS-553 (50Zr-30V-20Cb).

Studies on the effect of brazing parameters and testing variables on joint re-melt temperature ~~have been~~ were continued. The applied stress during testing was the most important variable in control of failure temperature.

The new braze alloys for tungsten were evaluated for melting range. Two alloys, AS-562 (70Cb-25V-5Si) and AS-564 (55Ta-40V-5Si), with suitable flow characteristics were examined metallographically. Severe braze cracking was observed, thus negating further investigation of these alloys. The selected braze alloys previously applied to ~~columbium~~ niobium-base alloys will be evaluated with tungsten.

cont'd, iv

Part II - Tungsten Alloy Ductility Improvement

Progress in three areas of experimental effort is described. Electron beam melted ingots of W-Hf and W-Hf-C alloys ~~have been~~ successfully worked to sheet. Gross thermal response characteristics ~~have~~ been established and tests to determine transition temperatures in the wrought, fully recrystallized, and fusion welded conditions ~~have been~~ initiated.

Further measurements of the grain boundary and bulk microhardness in several alloys were completed. No evidence of significant grain boundary hardening was observed in traverses made with symmetrical, randomly oriented indenters. The results demonstrate that earlier indications of grain boundary hardening were in fact related to a rather large hardness anisotropy.

Annealing of unalloyed tungsten in a carbon-free, ultra-high vacuum environment improves the low-temperature ductility. As the initial annealing temperature increased from 3000°F to near the melting point, the bend transition temperature of subsequently worked and fully recrystallized sheet was reduced from 425 to 275°F.

Part III - Diffusion Bonding Studies

The tensile shear strength of lap joints diffusion bonded between ~~(1) Cb~~ Nb-1Zr and 316 SS, ~~(2)~~ ~~Cb~~ Nb-1Zr to Cu, and ~~(3)~~ Cu to 316 SS ~~has been~~ determined. Both of the couples in which Cu is a component exhibit high bonding strength at room temperature and -100°F. This high strength is attributed to solution strengthening and absence of brittle intermetallic formation at the bonding interface. In contrast, the hard intermetallic layer formed in the Cb-1Zr/316 SS system led to bond-interface failure between room temperature and 1800°F. It is evident, however, that the ductility and hence the load-carrying capacity of the joint increases with temperature.

Additional experiments ~~have~~ confirmed the actual bonding between Be and 316 SS. Diffusion of Be into 316 SS, however, results in an extremely brittle joint.

The effect of Cr as a diffusion barrier in the Mo-0.5 Ti/R-41 and Mo-0.5 Ti/L-605 systems ~~has been~~ investigated. The barrier appears to have reduced the intermetallic diffusion and the attendant brittleness in Mo-0.5 Ti/R-41. Its effectiveness in Mo-0.5 Ti/L-605, however, has not been conclusively established.

PART I - BRAZING ALLOY SYSTEMS FOR COLUMBIUM AND TUNGSTEN

(W.R. Young - Responsible Engineer)

A. BRAZE ALLOY DEVELOPMENT - COLUMBIUM ALLOYS

A. 1. Higher Strength Alloys

All the braze alloys for this phase of the program have been evaluated for melting range, flow characteristics, and compatibility with base metals as determined by metallographic examination and hardness traverses. Results are presented in summary data sheets for each alloy (Figures 1 through 14) and summarized in Tables I and II.

From a study of these data and past experience with the binary alloys, the following observations can be made:

A. 1. a. For Service With F-48 Alloy To 2500°F

Titanium Base Alloys: AS-543, AS-544, AS-545

Although the melting range, wettability, and compatibility of these alloys were satisfactory, both metallographic examination and hardness traverses revealed the formation of a hard, presumably brittle, second phase during thermal exposure at 2500°F/10 hours. Because of this instability, these alloys were not selected for further evaluation.

TABLE I

BRAZE ALLOY SELECTION CRITERIA

Base Alloy F-48

Property	AS-540 60V-30Cb-10Ti	AS-541 60V-30Cb-10Ti+.2C	AS-542 59V-29Cb-10Ti-.2Si	AS-543 60Ti-27.5Cb-12.5V	AS-544 60Ti-27.5Cb-12.5V-.2C	AS-545 59Ti-26.5Cb-12.5V-2Si	AS-546 60V-30Cb-10Zr	AS-547 59V-29Cb-10Zr-2Si
Melting Range								
Solidus	3200	3200	3000	3100	3100	2900	3000	2000
Liquidus	3300	3300	3200	3300	3300	3000	3200	3100
Wettability	31°	28°	13°	46°	34°	13°	11°	8°
Compatibility								
Base Metal Erosion -As Brazed	.001"	.0005"	.002"	.0015"	.001"	.0005"	.001"	.000"
Diffusion Reactions 2500°F/10 hrs.	.001"	.0005"	.002"	.0015"	.0015"	.0015"	.0015"	.0005"
Knoop Hardness								
As Brazed	455-555	380-480	590-530	310-460	300-595	350-390	230-370	220-460
Heat Treated 2500°F/10 hrs.	530-450	510-630	410-750	540-690	530-920	500-2690	360-550	200-575

TABLE II

BRAZE ALLOY SELECTION CRITERIA

Base Alloy Cb-1Zr

Property	AS-548 30Zr-50V-20Ti	AS-549 50Zr-20V-30Ti	AS-550 30Zr-20V-50Ti	AS-551 40Zr-30V-30Ti	AS-552 30Zr-35V-35Ti	AS-553 50Zr-30V-20Cb
Melting Range						
Solidus	2400	2300	2500	2200	2400	2200
Liquidus (within 200°F of solidus)	2600	2400	2600	2300	2600	2300
Wettability Contact Angle	10°	25°	20°	14°	19°	15°
Compatibility						
Base Metal Erosion	.003"	.0015"	.001"	.0005"	.003"	.0005"
Diffusion Reactions 2200°F/5 hrs.	.006"	.006"	.005"	.0045"	.005"	.003"
Knoop Hardness						
As Brazed	210-390	250-410	350-400	250-630	260-460	260-720
Heat Treated 2200°F/66 hrs.	450-500	300-470	510-2470	440-510	210-590	390-810

Vanadium Base Alloys

The five vanadium-base alloys investigated, AS-540, 541, 542, 546, and 547, were designed to study the effect of Zr, Ti, Si, and C additions, and combinations thereof, to the V-35Cb binary system.

Zirconium is a more potent temperature depressant for the V-Cb binary than titanium, decreasing the liquidus from 3400 to 3200°F at the 10 W/O level. Similar titanium additions resulted in a 100°F decrease in liquidus temperature. The addition of 2 W/O silicon reduced the liquidus by an additional 100°F.

The addition of 0.2 W/O carbon to the V-Cb-Ti ternary produced considerable carbide precipitation and probably strengthening as illustrated by a comparison of Figures 1 and 2.

Alloy Selection

Of the five vanadium-base alloys evaluated (Table I), only AS-542 (59V-29Cb-10Ti-2Si) can be eliminated from further consideration. This alloy produced the most erosion (.002 inch) of the base alloy, and a hardness increase to > 600 Knoop during thermal exposure.

The four remaining alloys, AS-540, AS-541, AS-546, and AS-547, exhibited acceptable properties. These alloys have been selected for further screening by tensile-shear tests at 500 and 2500°F.

A. 1. b. Alloys For Service With Cb-1Zr Alloy At 1800 To 2200°F

The braze alloys for service with Cb-1Zr (Table II) were based on the ternary systems Zr-V-Ti and Zr-V-Cb. The purpose of these alloys was two-fold: (1) to identify alloys with solidus temperature above 2400°F to satisfy 2200°F service requirements, and (2) to further document the solidus/liquidus relationships in the ternary Zr-V-Ti system.

The summary of braze alloy properties tabulated in Table II reveals a most serious deterrant to the utilization of these alloys, that is, excessive erosion of the base alloy during prolonged thermal exposure at 2200°F. This continued solid state diffusion and resulting interface movement was not observed during previous 1800°F thermal exposure of AS-537 (Zr-28V-16Ti) alloy.(1).

The growth of this diffusion layer is illustrated in Figure 14 for the AS-553 (Zr-30V-20Cb) alloy.

Alloy Selection

Since none of the alloys investigated fulfill the goals for 2200°F service, only one alloy, AS-553 (50Zr-30V-20Cb), has been selected for strength determination at the minimum service temperature of 1800°F. This alloy will thus provide a strength comparison between the Zr-V-Cb ternary and the previously evaluated Zr-V-Ti (AS-537) ternary alloy.

Referring to AS-553 alloy (Figure 14), it should be noted that the diffusion layer produced at the braze/base alloy interface is considerably softer than the remaining braze alloy. This suggests that further exploration of this ternary system at intermediate zirconium levels, i.e., 20 to 30 W/O, may produce ductile alloys with melting ranges commensurate with 2200°F service requirements. This approach will be considered in future work.

A. 2. High Remelt Temperature Alloys

A. 2. a. Hetrogeneous Powder Additions

The AS-501 (Ti-30V) alloy with additions of columbium powder was selected to establish experimental procedures in determination of remelt temperatures. Initially, Cb-1Zr lap specimens were brazed with AS-501 alloy at 3000°F without powder additions and tested for remelt temperature by induction heating to failure under 4 psi static stress. Observed variations in failure mode and temperature necessitated a more sophisticated test procedure, involving more accurate temperature measurement. This has been accomplished in the past quarter.

The principal features of this procedure were: (1) resistance heating of the specimen, (2) black-body conditions for optical pyrometry are provided by .020 inch diameter holes drilled in the edge of the specimen, and (3) a special lens for the pyrometer which magnifies the .020 inch diameter black-body hole to twice the width of the pyrometer filament, thus allowing direct observation of the specimen.

To obtain data on temperature distribution for an overlap specimen, six black-body holes were drilled as shown schematically here:

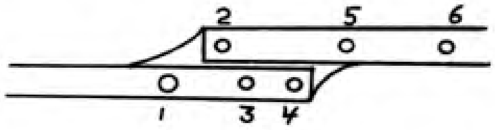

The data from temperature surveys are indicated in the following table. A maximum temperature gradient of about 100°F was observed within the brazed area of the joint.

Black-Body Hole No.	Temperature, °F		
	Test #1	Test #2	
1	2140	3000	
2	2100	2920	
3	2100	2905	Braze Area
4	2140	2920	
5	2150	2960	
6	2190	3030	

Actual remelt tests were performed with a tensile-shear stress applied to the specimen through a spring-loaded molybdenum holder. Power to the specimen was increased uniformly until separation occurred.

The time from stabilization at 2500 to 3000°F to failure temperature was less than 60 seconds. Specimen temperature was monitored continuously with the optical pyrometer during the heating cycle.

Utilizing this procedure, the failure temperatures of brazed joints under varying conditions of braze time, thermal exposure, columbium powder addition, and specimen geometry were determined as tabulated in Table III. By comparison of the seven conditions tested, the following observations can be made:

(1) Stress: The stress applied during testing was the most important factor in determining failure temperature. Group 4 (Table III), for example, exhibited a 600°F increase in failure temperature upon decreasing the stress from 38.4 to 11 psi.

(2) Brazing Time (5 vs. 15 mins.): The alloys containing 20 W/O columbium powder exhibited a 100°F higher failure temperature for the 15 minute braze cycle (Groups 4 and 5). AS-501 alloy without powder additions (Groups 1 and 3) exhibited no increase.

(3) Columbium Powder Additions: No observed effect at 38.4 psi stress level.

(4) Post-braze Heat Treatment (2500°F/10 hrs.): Approximately 100°F increase in failure temperature in specimens both with

TABLE III

REMELT STUDY TEST RESULTS

Cb-1Zr Base/AS-501 (Ti-30V) Alloy Braze

Specimen Identification		Applied Stress (psi)	Time At 2500°F	2500°F To Failure	Failure * Temp., °F	Comments
1. Joint Type	Lap					
% Cb Powder	None	38.4	1 min.	25 sec.	3375	Braze Failure
Braze Time & Temp.	3000°F/5 min.					
Heat Treatment	None	11	3 min. 30 sec.	1 min. 30 sec.	3900	Specimen failed by overheating at support hole.
2. Joint Type	Lap					
% Cb Powder	None	38.4	1 min.	30 sec.	3460	Braze Failure
Braze Time & Temp.	3000°F/5 min.					
Heat Treatment	2500°F/10 hrs.	11	1 min.	10 sec.	3500	Braze Failure
3. Joint Type	Lap					
% Cb Powder	None	38.4	1 min. 5 sec.	29 sec.	3380	Braze Failure
Braze Time & Temp.	3000°F/15 min.					
Heat Treatment	None	36.4	1 min.	29 sec.	3480	Braze Failure
4. Joint Type	Lap					
% Cb Powder	20%	38.4	1 min. 20 sec.	25 sec.	3420	Braze Failure
Braze Time & Temp.	3000°F/15 min.	38.4	1 min.	28 sec.	3400	Braze Failure
Heat Treatment	None					
		11	1 min.	39 sec.	4000	Braze Erosion
		11	1 min.	35 sec.	4040	Braze Erosion

(continued)

TABLE III (cont.)

REMELT STUDY TEST RESULTS

Cb-1Zr Base/AS-601 (Ti-30V) Alloy Braze

Specimen Identification		Applied Stress (psi)	Time At 2500°F	2500°F To Failure	Failure Temp., °F *	Comments
5. Joint Type	Lap					
% Cb Powder	20%	38.4	1 min.	25 sec.	3290	Braze Failure
Braze Time & Temp.	3000°F/5 min.	38.4	1 min.	27 sec.	3280	Braze Failure
Heat Treatment	None					
6. Joint Type	Lap					
% Cb Powder	20%	38.4	1 min	32 sec.	3450	Braze Failure
Braze Time & Temp.	3000°F/5 min.	38.4	1 min.	30 sec.	3380	Braze Failure
Heat Treatment	2500°F/10 hrs.	38.4	1 min.	30 sec.	3380	Braze Failure
7. Joint Type	Miller-Peaslee	103	3 min. 10 sec.	20 sec.	3320	Braze Failure
% Cb Powder	20%					
Braze Time & Temp.	3000°F/15 min.	50	1 min.	23 sec.	3980	Specimen failed by overheating of P.M.

* Temperature as measured by optical pyrometer, not corrected to true temperature which is 50 to 100°F higher.

(Groups 5 and 6) and without (Groups 1 and 2) columbium powder additions.

(5) Specimen Geometry: The effect of specimen geometry, especially braze filleting, was determined by comparison of lap joints (Group 4) and Miller-Peaslee joints (Group 7). Each group was brazed with AS-501 alloy with 20% columbium addition at 3000°F/15 minutes. The joint without fillets (Miller-Peaslee) exhibited a failure temperature 600°F higher than filleted joints under equivalent shear stress. Since the method of braze alloy application differed for these specimens, further metallographic evaluation is necessary to better define process and geometric effects.

It should be emphasized that all reported temperatures refer to the failure temperature of the brazed joint, rather than the actual remelt temperature of the braze itself.

One could reason that the strong dependence of failure temperature on applied stress could occur as a result of slight inhomogeneities in the braze alloy which result in "islands" of differing melting point within the joint area. At low stress levels, those portions of the braze alloy which remain unmelted prevent failure of the joint. At higher stress levels, these areas fail, producing a narrowing of the range between remelt and failure temperature.

The significance of this work in terms of the program goals are thus:

(1) The hetrogeneous powder approach to obtain higher failure temperatures will not be pursued since only negligible benefit was derived.

(2) All future determination of failure temperatures will be conducted at stress levels which provide an accurate measure of true braze remelt temperature.

(3) Additional physical metallurgy evaluations of diffusion parameters are needed before accurate predictions of failure temperatures can be made.

A. 2. b. Alloy Development

The second approach in obtaining higher remelt temperature is the identification of braze alloys with greater potential for high remelt. These alloys are based on eutectic systems which melt at considerably lower temperature than the base metal.

The properties of the two alloys designed for this study are summarized in Figures 15 and 16. The severe cracking which occurred in the AS-557 (55Ti-25V-20Fe) alloy is depicted in Figure 15 and negated any further consideration of this alloy.

The second alloy, AS-558 (62Ti-30V-8Si), fulfills the requirements for both melting range and compatibility with the base alloy. This alloy will be further evaluated for remelt characteristics. In addition, the compatibility of this braze alloy with Cb-1Zr alloy will be determined to evaluate its potential for service at 2200°F.

B. BRAZE ALLOY DEVELOPMENT - UNALLOYED TUNGSTEN

B. 1. Evaluation Of Binary Alloy Systems

Tungsten specimens for tensile-shear strength tests were prepared by electro-polishing to remove contaminated surface layers. These specimens are currently being prepared for brazing with alloys AS-517 (Cb-2.2B) and AS-519 (Cb-20Ti).

B. 2. Braze Alloy Design

The purpose of this phase of investigation is to identify alloy systems possessing brazing temperatures near 3000°F, with remelt temperatures of 3500°F or above.

The melting characteristics of alloys designated for this study are summarized in Table IV. Only the alloys from the Cb-V-Si and Ta-V-Si systems exhibited melting ranges and flow characteristics suitable for this study.

TABLE IV

SUMMARY OF MELTING RANGE DETERMINATIONS ON BRAZE ALLOYS FOR TUNGSTEN

Base Metal	Braze Alloy	Nominal Composition (Wt. %)	Melting Range (°F)
W	AS-559	75Cb-21Cr-4Si	3000 Sol 3100 Liq
	AS-560	69Cb-23Cr-8Si	3100 Sol 3700 Liq
	AS-561	77.5Cb-20Cr-2.5B	3500 Sol 4000 Liq
	AS-562	70Cb-25V-5Si	3000 Sol 3100 Liq
	AS-563	72.5Cb-25V-2.5B	3500 Sol 4000 Liq
	AS-564	55Ta-40V-5Si	2900 Sol 3000 Liq
	AS-565	78Ta-20V-2.0B	3800 Sol 4000 Liq
	AS-566	58Ta-40V-2.0B	3500 Sol 4000 Liq

The metallographic examination of these alloys (Figures 17 and 18) revealed the extremely high hardness of the braze alloys which resulted in cracking during braze solidification.

Since braze alloy solidification shrinkage on the surface of the flat tungsten panels may introduce severe bending stresses, both lap and "tee" specimens were prepared to determine the effect of specimen geometry. Both joint types exhibited severe cracking in both the braze alloy and tungsten base metal.

Thus, silicon containing alloys have been dropped from further consideration. Instead, the selected braze alloys previously applied to columbium-base metals will be evaluated with tungsten.

BRAZE ALLOY

SUMMARY DATA SHEET

Base Metal: F-48

Braze Alloy Designation	Nominal Composition	Melting Range °F Solidus	Liquidus	Ductility As Cast
AS-540	60V-30Cb-10Ti	3200	3300	Ductile

Wettability -

Time	5 Min.
Temperature	3300F
Contact Angle	31°
Mag:	1.25X

Microstructure -
As Brazed 3300F/5 Min.

Y2662

Heat Treated 2500F/10 hrs.

Y2952

Hardness Traverse -
As Brazed (3300F/5 Min)

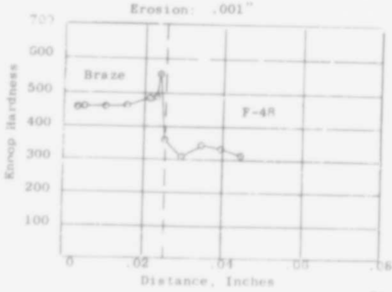

Heat Treated
(2500F/10 Hrs.)

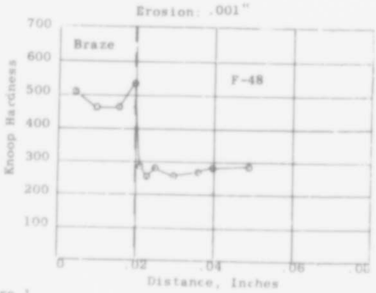

Figure 1

BRAZE ALLOY

SUMMARY DATA SHEET

Base Metal: F-48

Braze Alloy Designation	Nominal Composition	Melting Range °F Solidus	Liquidus	Ductility As Cast
AS-541	60V-30Cb-10Ti-.2C	3200	3300	Brittle

Wettability -

Time	5 Min.
Temperature	3300°F
Contact Angle	28°
Mag:	1.25X

Microstructure -
As Brazed 3300F/5 min.

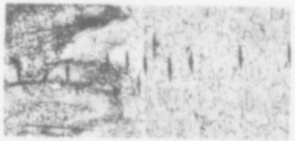

Y2663

Heat Treated 2500F/10 hrs.

Y3188

Hardness Traverse -
As Brazed (330F/5 min)

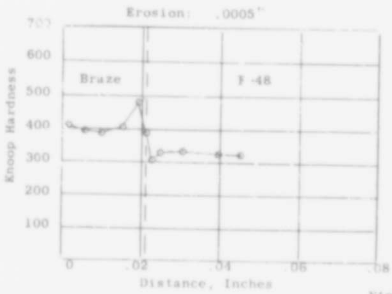

Heat Treated
(2500F/10 hrs)

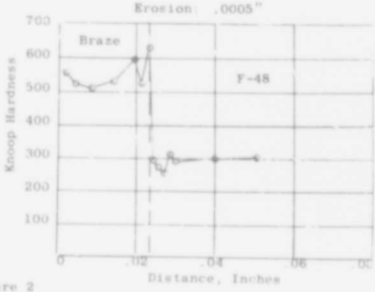

Figure 2

BRAZE ALLOY

SUMMARY DATA SHEET

Base Metal: F-48

Braze Alloy Designation	Nominal Composition	Melting Range °F Solidus	Melting Range °F Liquidus	Ductility As Cast
AS-542	59V-29Cb-10Ti-2Si	3000	3200	Brittle

Wettability -

Time 5 min.
Temperature 3200F
Contact Angle 13°
Mag: 1.25X

Microstructure -
As Brazed 3200F/5 min.

Y2947

Heat Treated +2500F/10 hrs.

Y3189

Hardness Traverse -
As Brazed (3200F/5 min)

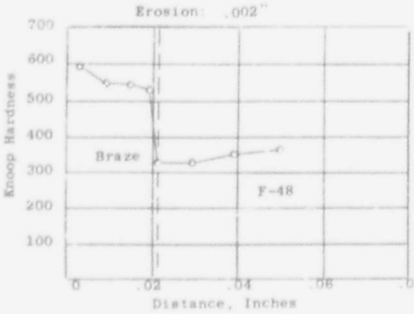

Heat Treated (2500F/10 hrs)

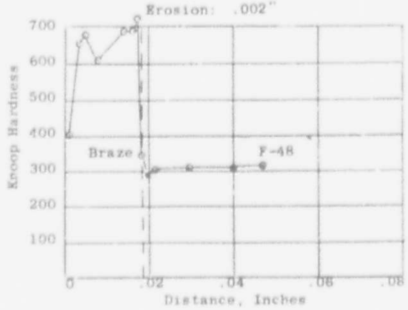

Figure 3

BRAZE ALLOY

SUMMARY DATA SHEET

Base Metal: F-48

Braze Alloy Designation	Nominal Composition	Melting Range °F Solidus	Melting Range °F Liquidus	Ductility As Cast
AS-543	60Ti-27.5Cb-12.5V	3100	3300	Ductile

Wettability -

Time 5 min.
Temperature 3200°F
Contact Angle 46°
Mag: 1.25X

Microstructure -
As Brazed 3200F/5 min.

Y2734

Heat Treated +2500F/10 hrs

Y3190

Hardness Traverse -
As Brazed (3200F/5 min)

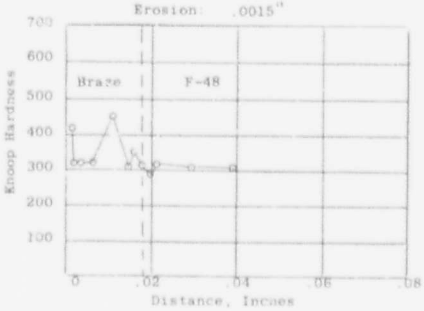

Heat Treated (2500F/10 hrs)

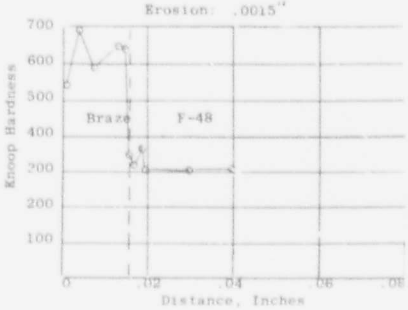

Figure 4

BRAZE ALLOY

SUMMARY DATA SHEET

Base Metal: F-48

Braze Alloy Designation	Nominal Composition	Melting Range °F Solidus	Melting Range °F Liquidus	Ductility As Cast
AS-544	60Ti-27.5Cb-12.5V-.2C	3100	3300	Brittle

Wettability -

Time 5 Min.
Temperature 3200F
Contact Angle 34°
Mag: 1.25X

Microstructure -
As Brazed 3200F/5 min.

Y2735

Heat Treated +2500F/10 hrs.

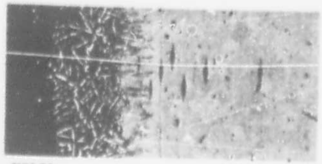

Y3191

Hardness Traverse -
As Brazed (3200F/5 min.)

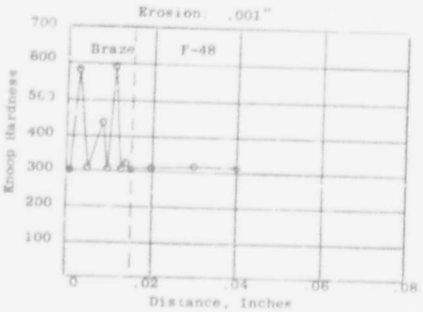

Heat Treated (2500F/10 hrs)

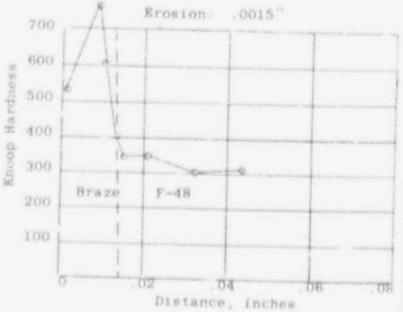

Figure 5

BRAZE ALLOY

SUMMARY DATA SHEET

Base Metal: F-48

Braze Alloy Designation	Nominal Composition	Melting Range °F Solidus	Melting Range °F Liquidus	Ductility As Cast
AS-545	59Ti-26.5Cb-12.5V-2Si	2900	3000	Brittle

Wettability -

Time 5 min.
Temperature 3000F
Contact Angle 13°
Mag: 1.25X

Microstructure -
As Brazed 3000F/5 min.

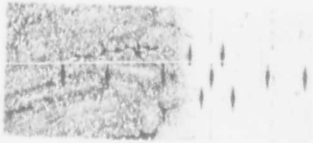

Y2948

Heat Treated + 2500F/10 hrs.

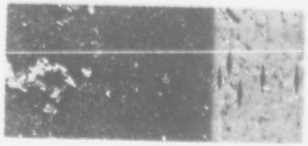

Y3192

Hardness Traverse -
As Brazed (3000F/5 min)

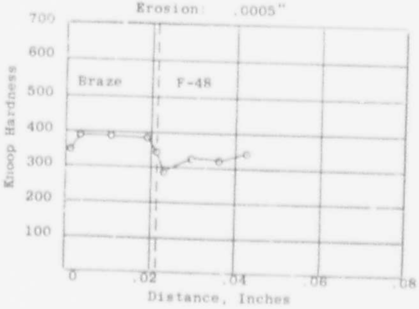

Heat Treated (2500F/10 hrs)

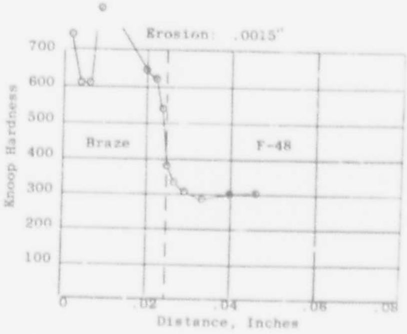

Figure 6

BRAZE ALLOY

SUMMARY DATA SHEET

Base Metal: F-48

Braze Alloy Designation	Nominal Composition	Melting Range °F Solidus	Melting Range °F Liquidus	Ductility As Cast
AS-546	60V-30Cb-10Zr	3000	3200	Brittle

Wettability -

Time 5 min.
Temperature 3200F
Contact Angle 11°
Mag: 1.25X

Microstructure -
As Brazed 3200F/5 min.

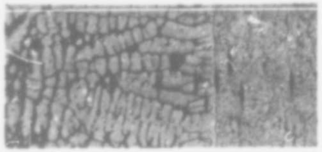

Y2736

Heat Treated 2800F/10 hrs)

Y3193

Hardness Traverse -
As Brazed (3200F/5 min)

Erosion: .001"

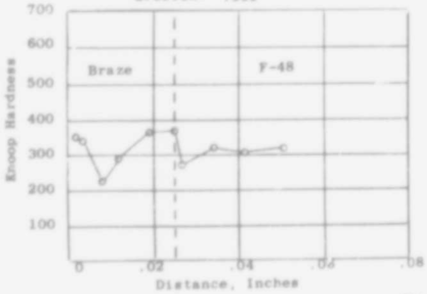

Heat Treated
(2500F/10 hrs)

Erosion: .0015"

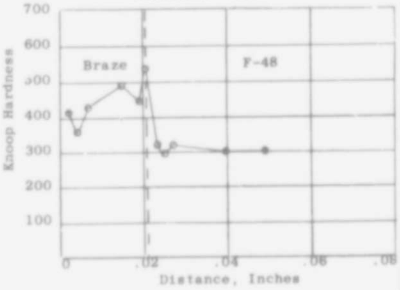

Figure 7

BRAZE ALLOY

SUMMARY DATA SHEET

Base Metal: F-48

Braze Alloy Designation	Nominal Composition	Melting Range °F Solidus	Melting Range °F Liquidus	Ductility As Cast
AS-547	59V-29Cb-10Zr-2Si	<2800	3100	Brittle

Wettability -

Time 5 min.
Temperature 3100F
Contact Angle 8°
Mag: 1.25X

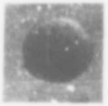

Microstructure -
As Brazed 3100F/5 min.

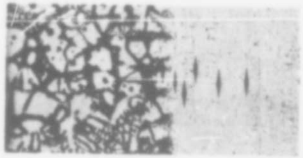

Y2949

Heat Treated + 2500F/10 hrs.

Y3194

Hardness Traverse -
As Brazed (3100F/5 min)

Erosion: None

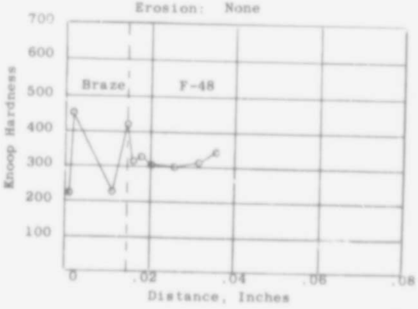

Heat Treated
(2500F/10 hrs)

Erosion: .0005"

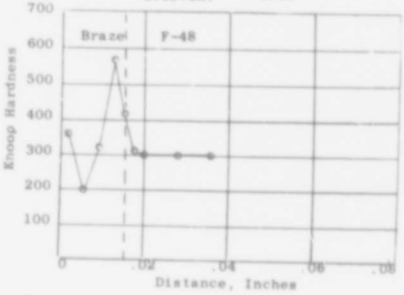

Figure 8

BRAZE ALLOY

SUMMARY DATA SHEET

Base Metal: Cb-1Zr

Braze Alloy Designation	Nominal Composition	Melting Range °F Solidus	Melting Range °F Liquidus	Ductility As Cast
AS-548	30Zr-50V-20Ti	<2400	2600	Slightly ductile

Wettability -

Time 5 min.
Temperature 2600F
Contact Angle 10°
Mag: 1.25X

Microstructure -
As Brazed 2600F/5 min.

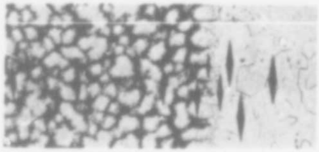

Y2938

Heat Treated + 2200F/65 hrs.

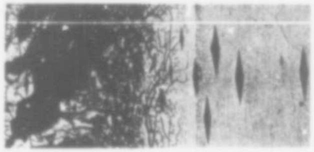

Y3195

Hardness Traverse -
As Brazed (2600F/5 min)

Erosion: .003"

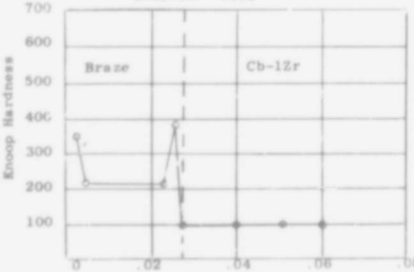

Heat Treated (2200F/65 hrs)

Erosion: .005"

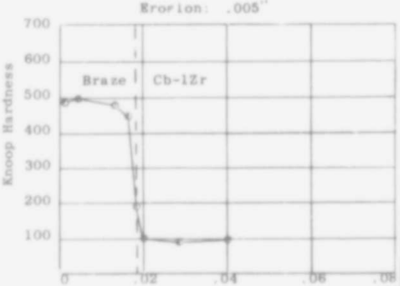

Figure 9

BRAZE ALLOY

SUMMARY DATA SHEET

Base Metal: Cb-1Zr

Braze Alloy Designation	Nominal Composition	Melting Range °F Solidus	Melting Range °F Liquidus	Ductility As Cast
AS-549	50Zr-20V-30Ti	2300	2400	Brittle

Wettability -

Time 5 min.
Temperature 2400F
Contact Angle 25°
Mag: 1.25X

Microstructure -
As Brazed 2400F/5 min.

Y2668 Y2940

Heat Treated +2200F/65 hrs.

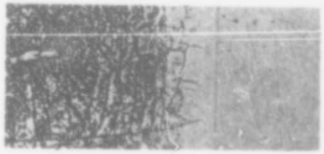

Y2670 Y2671

Hardness Traverse -
As Brazed (2400F/5 min.)

Erosion: .0015"

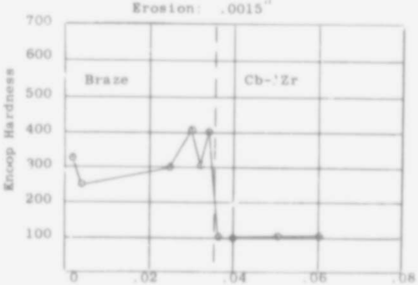

Heat Treated (2200F/65 hrs.)

Erosion: .006"

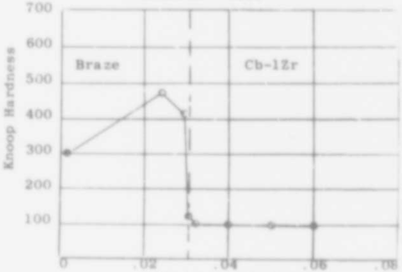

Figure 10

BRAZE ALLOY

SUMMARY DATA SHEET

Base Metal: Cb-1Zr

Braze Alloy Designation	Nominal Composition	Melting Range °F Solidus	Liquidus	Ductility As Cast
AS-550	30Zr-20V-50Ti	> 2500	2600	Slightly Ductile

Wettability -

Time 5 min.
Temperature 2600F
Contact Angle 20°
Mag: 1.25X

Microstructure -
As Brazed 2600F/5 min.

Y2941

Heat Treated 2200F/65 hrs.

Y3198

Hardness Traverse -
As Brazed (2600F/5 min)

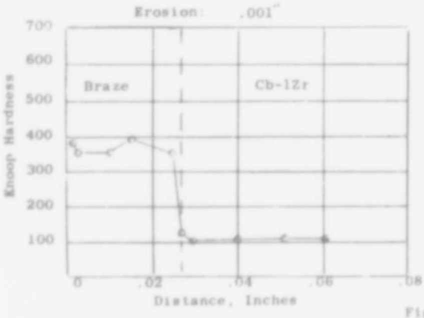

Heat Treated (2200F/65 hrs.)

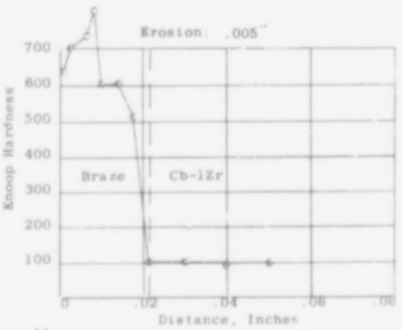

Figure 11

BRAZE ALLOY

SUMMARY DATA SHEET

Base Metal: Cb-1Zr

Braze Alloy Designation	Nominal Composition	Melting Range °F Solidus	Liquidus	Ductility As Cast
AS-551	40Zr-30V-30Ti	2200	2300	Brittle

Wettability -

Time 5 min.
Temperature 2300F
Contact Angle 14°
Mag: 1.25X

Microstructure -
As Brazed 2300F/5 min.

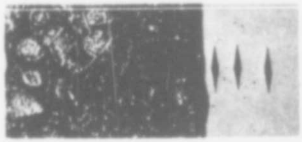

Y2943

Heat Treated + 2200F/65 hrs.

Y3200

Hardness Traverse -
As Brazed (2300F/5 min)

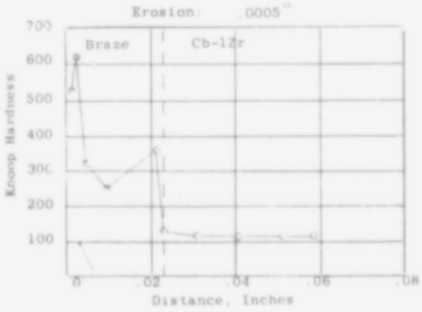

Heat Treated (2200F/65 hrs)

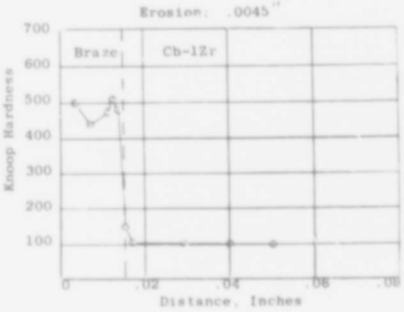

Figure 12

BRAZE ALLOY

SUMMARY DATA SHEET

Base Metal: Cb-1Zr

Braze Alloy Designation	Nominal Composition	Melting Range °F Solidus	Liquidus	Ductility As Cast
AS-552	30Zr-35V-35Ti	2400	2600	Brittle

Wettability -

Time	5 Min.
Temperature	2600F
Contact Angle	19°
Mag:	1.25X

Microstructure -
As Brazed 2600F/5 min. **Heat Treated** + 2200F/65 hrs.

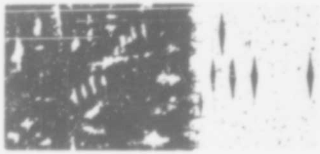

Y2944

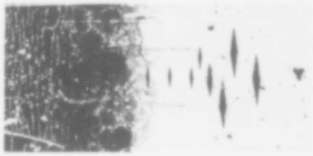

Y3201

Hardness Traverse -
As Brazed (2600F/5 min) **Heat Treated** (2200F/65 hrs)

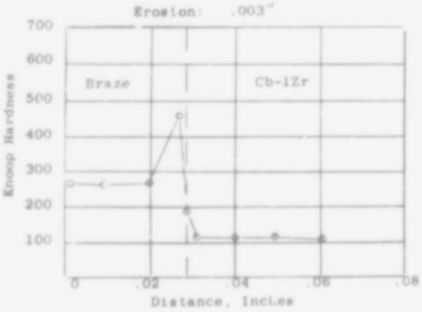

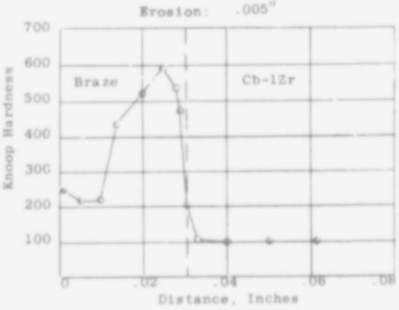

Figure 13

BRAZE ALLOY

SUMMARY DATA SHEET

Base Metal: Cb-1Zr

Braze Alloy Designation	Nominal Composition	Melting Range °F Solidus	Liquidus	Ductility As Cast
AS-553	50Zr-30V-20Cb	> 2200	2300	Very Brittle

Wettability -

Time	5 Min.
Temperature	2300F
Contact Angle	15°
Mag:	1.25X

Microstructure -
As Brazed 2300F/5 min. **Heat Treated** + 2200F/65 hrs.

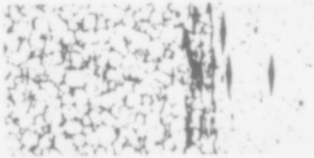

Y2945

Y3202

Hardness Traverse -
As Brazed (2300F/5 min) **Heat Treated** (2200F/65 hrs)

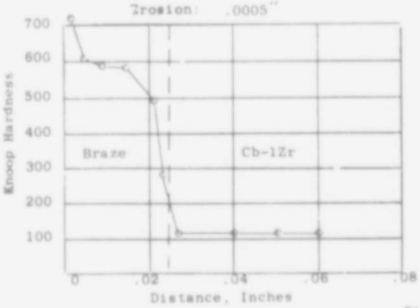

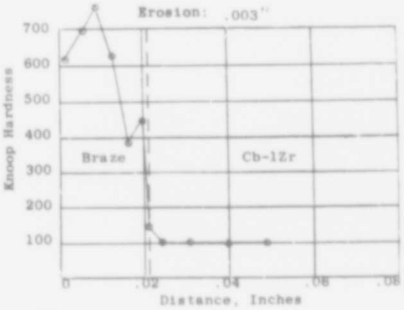

Figure 14

BRAZE ALLOY

SUMMARY DATA SHEET

Base Metal: F-48

Braze Alloy Designation	Nominal Composition	Melting Range °F Solidus	Liquidus	Ductility As Cast
AS-557	55Ti-25V-20Fe	2500	2600	Very Brittle

Wettability -

Time 5 min.
Temperature 2600F
Contact Angle 2°
Mag: 1.25X

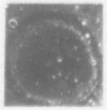

Microstructure -
As Brazed 2600F/5 min.

Y2946

Heat Treated + 2200F/65 hrs.

Y3203

Hardness Traverse -
As Brazed (2600F/5 min)

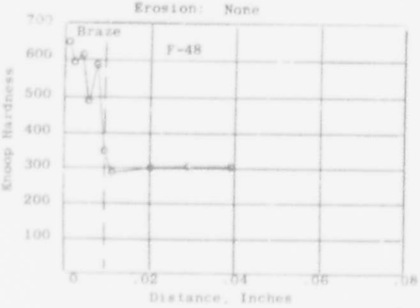

Heat Treated (2200F/65 hrs)

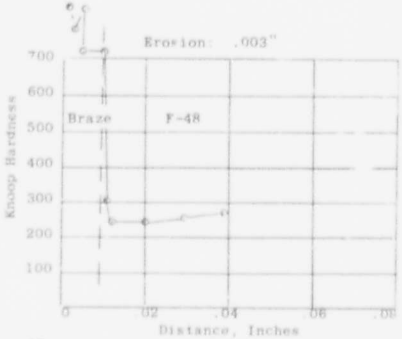

Figure 15

BRAZE ALLOY

SUMMARY DATA SHEET

Base Metal: F-48

Braze Alloy Designation	Nominal Composition	Melting Range °F Solidus	Liquidus	Ductility As Cast
AS-558	62Ti-30V-8Si	2300	2400	Very Brittle

Wettability -

Time 5 Min.
Temperature 2400F
Contact Angle 16°
Mag: 1.25X

Microstructure -
As Brazed 2400F/5 min.

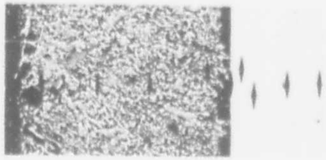

Y2950

Heat Treated +2200F/65 hrs.

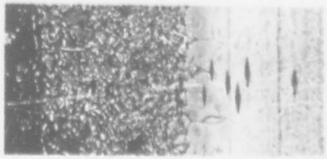

Y3204

Hardness Traverse -
As Brazed (2400F/5 min)

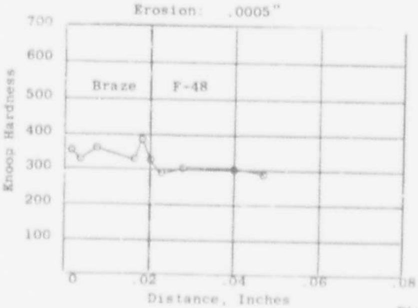

Heat Treated (2200F/65 hrs)

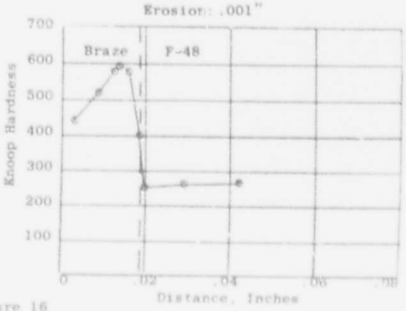

Figure 16

BRAZE ALLOY

SUMMARY DATA SHEET

Base Metal: W

Braze Alloy Designation	Nominal Composition	Melting Range °F Solidus	Liquidus	Ductility As Cast
AS-562	70Cb-25V-5Si	<3000	3100	Very Brittle

Wettability -

Time	5 Min.
Temperature	$3100^{\circ}F$
Contact Angle	2°
Mag:	1.25X

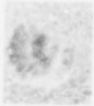

Microstructure -
As Brazed $3100^{\circ}F/5$ Min.   Heat Treated

Y3446

Hardness Traverse -
As Brazed $3100^{\circ}F/5$ Min.   Heat Treated

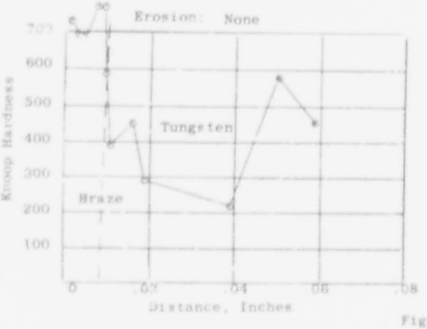

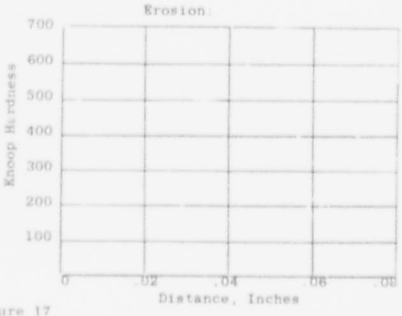

Figure 17

BRAZE ALLOY

SUMMARY DATA SHEET

Base Metal: W

Braze Alloy Designation	Nominal Composition	Melting Range °F Solidus	Liquidus	Ductility As Cast
AS-564	55Ta-40V-5Si	>2900	3000	Very Brittle

Wettability -

Time	5 Min.
Temperature	$3000^{\circ}F$
Contact Angle	5°
Mag:	1.25X

Microstructure -
As Brazed $3000^{\circ}F/5$ Min.   Heat Treated

Y3450

Hardness Traverse -
As Brazed $3000^{\circ}F/5$ Min.   Heat Treated

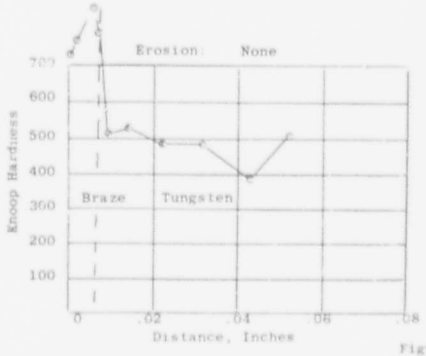

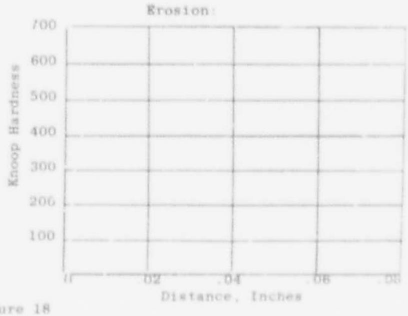

Figure 18

PART II - TUNGSTEN ALLOY DUCTILITY IMPROVEMENT

(J. W. Clark - Responsible Engineer)

Several recent investigations (2, 3, 4) have identified tungsten-base alloys which exhibit a ductile-to-brittle transition temperature superior to that of electron-beam melted, unalloyed tungsten in either the wrought, fully recrystallized, or fusion welded conditions. The most attractive compositions appear to be those which inhibit grain boundary embrittlement by impurities, either by promoting grain refinement or by altering the form and distribution of interstitial impurities. There are several independent indications that uncombined carbon has a particularly drastic effect on the low-temperature ductility of tungsten, even in the range of about 10 ppm, and that reduction of this concentration, or interaction of carbon with elements which form highly stable carbides such as the Group IV-A metals, tends to improve the low-temperature behavior.

The present work involves further study of the effects of compositional and microstructural variables on the low-temperature ductility of representative vacuum-melted alloy systems selected from earlier work. It also includes an exploratory effort to purify and thereby reduce the transition temperature of relatively massive forms of powder metallurgy tungsten by high-temperature annealing under ultra-high, carbon-free vacua.

A. ALLOY STUDIES

The characteristics upon which the selection of the present alloy series was based have been presented in some detail in the previous quarterly reports [(5)]. Electron-beam melting was chosen as the preferred method of consolidation of these alloys as approximately 4-pound ingots, since sheet produced from EB melted tungsten and tungsten-base alloys were shown earlier to have better low-temperature ductility than commercial powder metallurgy tungsten in either the fully recrystallized or, particularly, the fusion welded condition [(3)].

A.1. Alloy Preparation

Powder charges of each of ten compositions were twin-shell blended as two-kilogram lots, hydrostatically pressed at approximately 45,000 psi into cylindrical compacts and sintered for one hour in vacuum (10^{-5} torr) at 3700 to 3900°F. Gaseous impurities were removed by holding the charges at about 1800°F until the pressure dropped below 10^{-4} torr. The complete sintering cycle, including outgassing, required from 3 to 5 hours, depending on oxygen and hydrogen contents of the alloying additions. A significant pressure increase during final high-temperature sintering was observed only in the alloy containing 26% Re, indicating that not all of the volatile rhenium oxides were removed during the pre-sintering treatment. Sintered densities ranged from 78 to 86% of theoretical.

After a survey of potential melting sources and evaluation of trial EB melted ingots of unalloyed tungsten, the compacts were delivered to the organization selected, to be completed in March. Six of the alloys were melted and delivered to this laboratory in late May. Repeated equipment and/or scheduling difficulties made it impossible for the melting source to complete the remaining alloys by late July. Consequently, the latter compositions have been sent to the General Electric Research Laboratory for consumable electrode vacuum arc-melting. The furnace to be used in this work can be maintained at a pressure of about 10^{-5} torr during melting and it is equipped with a retractable ingot mold. These conditions are comparable to those employed in the earlier EB drip-melting. Since, in addition, the material is reduced in area by greater than 90% during ingot breakdown and subsequent sheet rolling, the differences in solidification structures produced in EB and arc-melting are not expected to bias the compositional variations under study.

The nominal compositions of the alloys are shown in Table V which includes the microhardness and grain size of the EB melted ingots. The compositions designated ACW-XX are those which are to be vacuum arc-melted.

The EB melted alloys were triple drip-melted in a 1.5" diameter mold. The ingots had irregular surfaces typical of EB melted tungsten, but the defects were relatively shallow and were removed by conditioning

TABLE V

COMPOSITION AND CAST PROPERTIES OF TUNGSTEN ALLOYS

Alloy Designation	Nominal Composition		Cast Hardness (VHN)	Grain Diameter (mm)
	Atomic %	Weight %		
EBW-21	1 Hf	1 Hf	363	5.7
EBW-22	2 Hf	2 Hf	341	4.2
EBW-23	5 Hf	5 Hf	355	3.7
EBW-24	1 Hf - .5 C	1 Hf - .033 C	373	1.3
ACW-25	2 Hf - 1 C	2 Hf - .066 C	-	-
ACW-26	3 Re	3 Re	-	-
ACW-27	26 Re	26 Re	-	-
ACW-28	.5 B	.030 B	-	-
EBW-29	1.5 B	.090 B	414	2.4
EBW-30	.25 Ru	.15 Ru	338	4.4

prior to extrusion. As shown in Table V, the grain size is quite large, with average grain diameters from greater than 1 to almost 6 mm. These values were measured on radial sections of the ingots. Since the solidification structure is decidedly columnar, the average dimensions in the axial direction are considerably greater than the diameters recorded in Table V.

In preparing the series of alloys studied previously in this program (3), final consolidation was performed by non-consumable EB melting as 2-inch diameter buttons. The more nearly non-directional freezing in that technique resulted in much finer equiaxed grain sizes in the range of 0.2 to 2 mm, such that ingot breakdown could be performed by upset forging. The very large columnar grain structure of the present alloys necessitated a less severe initial working operation. Consequently, ingot breakdown of these alloys was accomplished by extrusion.

Each of the ingots was machined and ground to 1-inch diameter, then sectioned into two equal lengths of about 1.5" for extrusion. Four of the alloys (EBW-21 through EBW-24) have been impact extruded to rectangular sheet-bar. A die failure delayed the remaining two, which will be extruded with the arc-melted compositions when the latter are completed. It required approximately 30 seconds to heat the conditioned billets to the extrusion temperature of 3000°F in an argon blanketed induction coil. They were held at this temperature for 15 seconds and then transferred, with handling times of 6 seconds or less, to a fast-acting vertical press and extruded through rectangular die inserts to a cross-section of 0.7" by 0.45", a reduction ratio of approximately 2.5 to 1. A 5-mil layer of ZrO_2 was flame-sprayed on the expendable die inserts in order to minimize die wash and improve surface quality of the sheet bars. The large columnar grain structure of the EB melted ingots was not greatly refined by extrusion at this relatively small reduction ratio. In most cases, there was some grain boundary separation in the nose of the extrusion, but such defects were confined to a depth of less than 0.5".

After cropping, hand-grinding, and polishing to remove major surface imperfections, the sheet-bars were rolled to .050" strip. They were rolled from the initial thickness of about 0.4 to 0.15" at 2400°F, taking a reduction of approximately 10% per pass. At a thickness of .15", the slabs were fully recrystallized by a one-hour anneal at 3000°F in vacuum and were then rolled at 2000°F to the final thickness of .050", again taking 10% reductions. Although there was slight lamination and longitudinal splitting of some sections of strip from each alloy, these cracks were confined to the ends. No edge cracking occurred in any of the compositions and the major portion of each was of excellent quality.

A. 2. Softening, Recrystallization, And Grain Growth

Small sections of each alloy were vacuum-annealed in the range of 2000 to 4000°F (1100 to 2200°C). The hardness and microstructural characteristics are summarized in Table VI.

The thermal response of the three binary Hf alloys is quite similar. Increasing the Hf concentration from 1 to 5% changes the one-hour recrystallization temperature by no more than 100°F. Each of the W-Hf alloys shows initial recrystallization at 2750 ± 50°F and is fully recrystallized at 3000°F. There is a slight but consistent refinement of the annealed grain size as the Hf content is increased. After annealing in the range 3000 to 4000°F, the mean grain diameters, measured by the line intercept technique, are 20 to 30% smaller in the 5% Hf than in the 1% Hf alloy.

However, as was the case in smaller heats studied in earlier work(3), a much larger effect on thermal response characteristics results upon addition of C to the dilute W-Hf composition. The recrystallization temperature is raised by 200 to 250°F and the annealed grain diameter of the 1Hf-.033C alloy are less than half as large as those in the comparable binary.

TABLE VI

THERMAL RESPONSE OF ELECTRON BEAM MELTED TUNGSTEN ALLOYS

Alloy Designation	Nominal Comp. (Wt. %)	1-Hr. Annealing Temp. (°F)	Hardness (DPH)	Grain Dia. (mm)
EBW-21	W - 1 Hf	As Rolled	501	W [(a)]
		2500	475	W
		2750	453	20% RX
		2875	380	80% RX
		3000	379	.065
		3250	379	.10
		3500	376	.197
		4000	362	.67
EBW-22	W - 2 Hf	As Rolled	499	W
		2500	485	W
		2750	481	5% RX
		2875	427	40% RX
		3000	392	.060
		3250	389	.084
		3500	375	.167
		4000	360	.575
EBW-23	W - 5 Hf	As Rolled	527	W
		2500	481	W
		2750	469	W
		2875	425	20% RX
		3000	371	.055
		3250	373	.074
		3500	376	.122
		4000	381	.465
EBW-24	W - 1Hf - .033C	As Rolled	543	W
		2500	536	W
		2750	507	W
		2875	487	5% RX
		3000	412	80% RX
		3250	383	.039
		3500	372	.099
		4000	344	.305

(a) Wrought structure

A. 3. Low-Temperature Ductility

These alloys are currently being bend tested in the wrought, annealed, and electron-beam welded conditions. Specimen preparation and testing techniques have been described in detail elsewhere (3). Test coupons with dimensions of 1.5" by 0.35" were electropolished at about 10 volts and 6 amps/in^2. in a solution of NaOH : $NaNO_2$: H_2O in the ratio 1 : 14 : 40 by weight. Bend tests were conducted in a circulating air oven mounted on an Instron frame. Three-point loading tests were made in a 75° V-block, using a bend radius of approximately four times the sheet thickness and a ram speed of .05 ipm. Initial results are summarized in Table VII.

The values recorded are the results observed in a single series of tests at decrements of 50°F in the temperature range 550 to 200°F. The indication of a relatively low bend transition temperature of the W-1Hf-.033C alloy in the wrought condition is promising, but the initial results obtained in the coarser-grain (annealed or welded) conditions of this composition are somewhat higher than comparable values observed previously in this program (3). Since it is planned to make duplicate or triplicate tests of these alloys in each condition, and several other alloys have yet to be evaluated, it is not felt that further comparison with earlier data is warranted at this time.

TABLE VII

BEND DUCTILITY OF ELECTRON BEAM MELTED TUNGSTEN ALLOYS

Alloy	Nominal Comp. (Wt. %)	Condition	4T Bend Transition Temp. (°F)
EBW-21	W - 1 Hf	Stress relieved (a)	300
		Annealed (b)	425
		EB Welded (c)	400
EBW-22	W - 2 Hf	Stress relieved	350
		Annealed	450
		EB Welded	400
EBW-23	W - 5 Hf	Stress relieved	325
		Annealed	500
		EB Welded	425
EBW-24	W - 1Hf - .033C	Stress relieved	225
		Annealed	500
		EB Welded	475

(a) Rolled 67% at 2000°F, stress relieved at 2400°F/1 hr.

(b) Rolled and annealed at 3500°F/1 hr.

(c) EB welded and stress relieved at 2000°F/1 hr.

A. 4. Grain Boundary Hardness

In the previous quarterly report (5), some evidence of grain boundary hardening in relative pure EB melted tungsten was reported. The hardness measurements were made with a diamond-based pyramid (Knoop) indenter, using 10 and 25 gram loads. Although these conditions could have been the source of some error, the shape of the indenter and the low loads were selected in order to space impressions a few microns apart without overlapping the strain fields. The fact that other bcc metals display a marked hardness anisotropy, with a strong dependence upon the orientation of the indenter with respect to crystallographic directions in the grain, had also been considered earlier (5). It was felt that the practice of averaging at least three randomly oriented traverses across a single grain would tend to minimize the expected orientation dependence. One other possible source of inconsistency was that the measurements were made in a welded sample (chosen because of the relatively large grain size). The specimen had been stress-relieved at 2000°F after welding, but the rapid cooling rates during welding could have caused some localized internal stresses which might not have been removed in the post-weld anneal.

Under these conditions, the average of several individual microhardness traverses across single grains in the fusion zone of an electron-beam weld bead in unalloyed tungsten indicated that regions within about

40 microns of the boundary were harder than the bulk of the grain by as much as 25%. Although this was the general trend, it was also reported that a few of the averaged traverses across a grain revealed no significant hardness differences and some individual traverses showed the boundary to be softer than the interior of the grain. Since no direct conclusions could be drawn from such divergent data, and since the technique appeared to be valuable in providing additional characterization of grain boundary conditions in a material in which low-temperature fracture is intergranular in origin, further work has been undertaken to investigate the factors in the foregoing discussion. Both a welded and stress-relieved sample and a non-welded sample annealed at 4350°F (2400°C) were selected from each of four EB melted alloys from the earlier study(3), unalloyed W, W-1Hf, W-.033C, and W-1Hf-.033C. Hardness was measured across and along grain boundaries in at least three different locations, using both the Knoop and the square-based diamond pyramid (Vickers) indenter and a load of 50 grams. At least 40 impressions were made in each case. The results are summarized in Table VIII.

In none of the present samples is there any marked difference between the hardness of the boundary and that of the bulk of the grain. The one result which is consistent in each sample is the extremely wide scatter in the Knoop hardness data. Although no attempt was made to define the crystallographic orientation of the grains, it would appear that this

TABLE VIII

GRAIN-BOUNDARY AND BULK MICROHARDNESS OF SELECTED TUNGSTEN ALLOYS

Alloy Designation	Nominal Comp. (Wt. %)	Condition [a]	Knoop Hardness				Vickers Hardness			
			Grain Boundary		Bulk		Grain Boundary		Bulk	
			Avg.	Δ KHN [c]	Avg.	Δ KHN	Avg.	Δ VHN [c]	Avg.	Δ VHN
EBW-1	Unalloyed W	EB Welded[b]	516	156	431	183	-	-	-	-
EBW-1	Unalloyed W	EB Welded	474	71	469	124	354	36	348	42
		Annealed	472	106	498	109	383	62	389	60
EBW-4	W - 1 Hf	EB Welded	455	193	467	181	374	42	385	37
		Annealed	442	120	444	148	368	38	377	56
EBW-9	W - .033 C	EB Welded	504	160	477	257	353	51	349	42
		Annealed	523	113	527	131	365	53	363	46
EBW-11	W - 1Hf - .033C	EB Welded	477	104	438	118	369	46	363	37
		Annealed	446	92	463	102	362	58	369	77

(a) Conditions: Electron beam welded .050" sheet, stress-relieved at 2000°F/1 hr.
Sheet annealed at 4350°F (2400°C) - 1 hr.

(b) Previous data (5) at 10 and 25 gram load. All others 50 gram load.

(c) Hardness difference between highest and lowest values.

scatter is due to a large hardness anisotropy of tungsten crystals. This of course would be much more evident in Knoop than in Vickers impressions since the ratio of the long to the short axes of the former indenter is about 7 to 1 while the latter is equiaxed and the diagonal readings are averaged in the determination of the dimensions of the impression. It is concluded that the earlier indication of grain boundary hardening is merely accidental, due to the orientation of the specific grains surveyed or the orientation mismatch across their boundaries. It also appears that non-symmetrical indenters such as the Knoop should not be used to measure the microhardness of materials in which the possibility of hardness anisotropy exists.

B. HIGH-VACUUM ANNEALING

Trace gaseous or metallic impurities may well be the critical factors in the low-temperature brittleness of polycrystalline tungsten. However, as discussed previously (3, 5), there is evidence that carbon in solution, even at low concentrations, has a large embrittling effect. It is difficult to reduce the carbon concentration to levels below about 10 ppm by conventional vacuum techniques. This difficulty stems in part from the nature of the environment produced in the usual method of attaining high vacua. Most of the studies of the effects of purity on mechanical properties, including the present series of alloys, have employed high-

temperature annealing, arc- or electron-beam melting, or zone refining in vacua produced by oil diffusion pumps. Regardless of precautions such as baffles or cold traps, there can be a small but finite concentration of carbon or hydrocarbons in the atmosphere. The carbon level in a specimen being annealed in this type of system can only be reduced to a value in equilibrium with the environment. In fact, evidence of carbon-enrichment during repeated zone refinement of tungsten has been reported (6).

In the present work, several powder metallurgy tungsten rods have been self-resistance heated in a vacuum produced by a multi-cellular getter-ion pump of the sputtering type (7). This facility is capable of maintaining pressures at least as low as 10^{-8} torr. Since initial evacuation is accomplished by liquid nitrogen absorption pumps, there is no source of carbon in the system. Ten-inch long rods of 0.125" diameter were heated at temperatures from 3000°F to near the melting point for periods of several hours and one 0.25" diameter rod was heated to an equilibrium temperature of about 3500°F at maximum power input (which is dictated by ceramic-to-metal seals on the high-current leads). Identical rods were also radiation-heated at 3500°F in a vacuum of 10^{-4} to 10^{-5} torr in a system evacuated by oil diffusion pumps, to provide base-line data. Vacuum fusion, combustion-conductometric and spectrographic analyses of the initial rod (General Electric Lamp Metals, Lot MK-131) gave the following results, in ppm by weight:

O	N	H	C	Total Metallics	W
58	1	1	12	150	Balance

After annealing, the rods were rolled to approximately .040" strip at 2000°F, heating in dry H_2 with a dew point of -90°F. The wrought strip was then electropolished in the $NaNO_2$-NaOH solution, wrapped in Ta foil, and fully recrystallized by annealing at 3000°F for 1/2 hour under conventional vacuum of 10^{-5} torr. Specimens for bend testing were taken from strip produced from the center 6" sections of the rods, over which the initial temperature was quite uniform. At least two specimens from each condition were bent at temperature intervals of 50°F in the range of 500 to 250°F, using the procedures reported in a previous section. The average transition temperatures observed are recorded in Table IX which includes a summary of the initial annealing cycles of the rods (5) and the final grain size and hardness of the recrystallized strip.

The transition temperature of the recrystallized strip produced from 1/8" rods which were resistance-heated in ultra-high vacuum decreases from 425 to 275°F as the annealing temperature is raised from about 3000 to 5750°F. Since there was little structural difference in the fully recrystallized strip, the results suggest that the improvement may have resulted from removal of a minor impurity. Interstitial analyses of

TABLE IX

BEND DUCTILITY OF TUNGSTEN AS FUNCTION OF VACUUM ANNEALING CONDITIONS

Specimen (a)	Initial Annealing Conditions Temp. (°F)	Time (min.)	Pressure (torr)	Recrystallized Strip (b) VHN	Grain Dia. (mm)	Yield Strength at 450°F (Ksi)	4T Bend Transition Temperature (°F)
4-0	3500	200	2×10^{-5}	351	.044	80.0 *	400
8-0	3500	200	1×10^{-5}	361	.044	74.8 *	425
4-1	3490	200	1×10^{-7}	352	.037	77.0 *	350
8-1	3020	500	2×10^{-9}	354	.037	71.5 *	425
8-2	4250	250	8×10^{-9}	358	.046	69.4	400
8-3	5020	50	8×10^{-8}	363	.038	66.7 +	350
8-4	5750	200	6×10^{-8}	356	.050	58.7 +	275

(a) 0.25" dia. (4-X) and 0.125" dia. (8-X) powder metallurgy tungsten rods.

(b) Annealed rods rolled to .040" strip, recrystallized at 3000°F/$\frac{1}{2}$ hr.

* Distinct yield point

\+ Continuous yield

representative annealed samples are currently in progress. However, if removal of carbon is the critical factor as postulated, it is not likely that these analyses will establish the differences in carbon content since the as-received concentration is near the limit of detectability.

There is some indirect evidence that purification has occurred. The minimum chamber pressures, although extremely low in each case, increased by a factor of 30 to 40 as the temperature of the rods was raised from 3000 to above 5000°F. In addition, the yield strengths, compared in Table IX at 450°F (the lowest temperature at which all specimens were ductile), decrease with increasing annealing temperature. The distinct yield points which appear in the control samples, and in those annealed in the sputter-ion vacuum system at temperatures below 5000°F, are not observed in the strips which had been annealed at the two highest temperatures. Since earlier data had suggested that yield point phenomena in this temperature range are more closely associated with carbon than with oxygen concentration (3), the absence of a yield point in the latter samples with identical processing and thermal history after ultra-high vacuum annealing may be indicative of carbon removal.

Although they are outside the scope of the present work, techniques such as the use of a sensitive mass spectrometer during annealing or measurement of resistivity and internal friction characteristics should yield a quantitative estimate of the degree of purification. Pending the

results of interstitial analyses and detailed fractographic examination now in progress, it may be possible to briefly explore one or more of these techniques.

PART III - DIFFUSION BONDING STUDIES

(The late E. S. Jones - Responsible Engineer)

The third portion of this project pertains to an exploratory investigation of diffusion bonding as a technique for solid-state joining of dissimilar metals. In addition to examining the feasibility of achieving diffusion bonds between various classes of materials and studying the thermal stability of the bonding interfaces, this investigation also seeks to obtain preliminary data on the strength/ductility characteristics of diffusion-bonded joints of selected materials.

A. EXPERIMENTAL RESULTS

A. 1. Bond Strength Determination

Using previously-described joint design (5), a total of twelve tensile shear specimens were prepared from the three combinations of (1) Cb-1Zr to 316 SS, (2) Cb-1Zr to Cu, and (3) Cu to 316 SS. These combinations are attractive from systems standpoint and are not readily amenable to joining by welding or brazing owing to their great differences in melting point and/or thermal conductivity. Furthermore, the three combinations include one which forms an intermetallic at the interface (Cb-1Zr to 316 SS), one in which there is neither intermetallic nor extensive interdiffusion (Cb-1Zr to Cu) and one which forms a rather wide, ductile diffusion zone at the interface (Cu to 316 SS).

The shear specimens were diffusion bonded in vacuum of about 5×10^{-5} torr under the following conditions:

Specimen	Lap Material	Temp., °F	Time, Hr.
Cb-1Zr to 316 SS	Cb-1Zr	1800	4
Cb-1Zr to Cu	Cb-1Zr	1800	4
Cu to 316 SS	Cu	1800	2

The tensile-shear tests were conducted in an Instron machine, using a cross-head rate of 0.01 ipm. The test results are given in Table X and representative microstructural and hardness characteristics are shown in Figure 19 . Figure 20 shows tested specimens.

At room temperature, both of the couples in which copper is a component exhibited tensile failure in the copper rather than shear failure across the bonding interface. The Cu / Cb-1Zr specimen also failed by tensile fracture of the copper at -100°F, the bond sustaining a maximum shear stress of about 7,100 psi. As shown in Figure 19, neither the microstructure nor the hardness traverse of this joint suggests the formation of a brittle interface. Limited work on the Cb-Cu binary indicates a simple eutectic system (5) in which solid-state diffusion would not be expected to cause embrittlement. This is the type of bi-metal joint where diffusion bonding may be applied with more success than could other more common techniques. For instance, fusion welding of such a combination

TABLE X

TENSILE SHEAR DATA ON DOUBLE-LAP DIFFUSION-BONDED SPECIMENS

Specimen	Lap Material	Test Temp. °F	Location Of Failure	Max. Shear Stress On Bond (psi)
Cb-1Zr-316 SS	Cb-1Zr	R. T.	bond interface	10,730
		600	bond interface	11,480
		1200	bond interface	11,980
		1800	bond interface	4,180
Cb-1Zr-Cu	Cb-1Zr	R. T.	Cu sheet rupture	5,780
		-100	Cu sheet rupture	7,080
Cu-316 SS	Cu	R. T.	Cu laps rupture	14,730
		R. T.	Cu laps rupture	14,700
		-100	bond interface	15,970
		-100	bond interface	16,000

would be virtually impossible and brazing very difficult, because of the wide differences in melting point and thermal conductivity.

In contrast to its room-temperature failure, the Cu / 316 SS couple fractured at the bonding interface at -100°F. The joint, however, was able to support a relatively high shear stress, about 16,000 psi, prior to rupture at this temperature. None of the elements in 316 SS are known to form intermetallic compounds with Cu. The solid solubilities and interdiffusion coefficients at the bonding temperature are considerably greater than those in the Cb-Cu system, as indicated by the wide diffusion zone shown for the Cu / 316 SS couple in Figure 19. According to the hardness traverse, the strength of this zone should be intermediate between that of Cu and 316 SS. The fact that the joint actually failed at the bonding interface suggests that the failure may have been brought about by some bonding imperfections.

The Cb-1Zr / 316 SS joint forms a typical hard intermetallic layer (Figure 19) which apparently led to the brittle bond interface failure at room temperature. Additional specimens of this combination were tested at 600, 1200, and 1800°F. Bond fracture was encountered in all cases. However, with increasing temperature, both yielding of the parent materials and plastic flow within the diffusion-bonded region were observed. The increase in ductility and, hence, strength with temperature at the bond interface is also evidenced by the higher shear strength sustained at 1200°F than at 600°F and R. T. Even at the latter temperature, a significant shear stress was transmitted across the Cb-1Zr / 316 SS bond prior to fracture. These characteristics suggest the possibility, particularly at elevated temperatures, of inducing tensile failure in the parent materials by increasing the length of the overlap. In applications where impact loading is of no concern, diffusion bonding might be successfully utilized for the Cb-1Zr / 316 SS system, in spite of the intermetallic formation.

A.2. Additional Be Bonding Experiments

In accordance with previous planning, an additional attempt has been made to achieve a sound bond between Be and 316 SS. The diffusion couple was heated in vacuum at 1800°F for 4 hours, great care being taken in surface preparation and in removing the specimen from the bonding capsule after the diffusion treatment. Upon removal, the joint appeared intact. A photomicrograph of the joint is shown in Figure 21. The joint is seen to have fractured at the interface. It is not clear whether the fracture occurred during the metallographic preparation. There is, however, little doubt that bonding must have taken place, as evidenced by the extensive diffusion zone with its extremely high hardness near the 316 SS / Be interface. The brittleness of the diffusion zone is clearly indicated by the longitudinal cracks induced by the hardness impression. Thus, the present results indicate that while these two materials can be directly diffusion bonded together, the resulting brittleness may severely limit the load-bearing capability of the joint.

A. 3. Effect Of Diffusion Barrier

As shown in Quarterly Progress Report No. 4, diffusion bonding of Mo-0.5Ti to L-605 or R-41 resulted in the formation of brittle intermetallic layer. The effect of inserting a Cr barrier at the interface was investigated during the past quarter. A 0.001 in. layer of Cr was electroplated on both faces of a 1/2 in. dia. disc. of Mo-0.5Ti, which was sandwiched between polished L-605 and R-41 discs. The assembled couples were then heated in vacuum at 1800°F for 4 hrs. The resulting microstructures and hardness traverses are shown in Figures 22 and 23, together with previous results obtained at 1800 and 2000°F without Cr barrier. In the R-41 / Mo-0.5Ti system (Figure 22), it appears that the Cr layer has served as an effective barrier in limiting the intermetallic formation and the attendant brittleness. The effect of Cr barrier in the L-605 / Mo-0.5Ti couple is not so clear, as the joint fractured near the Cr / L-605 interface (Figure 23). The fracture may be due to poor quality of the Cr plating. Alternatively, a Cr-rich carbide layer may have formed along the Cr / L-605 interface, resulting from carbon diffusion out of L-605. This layer would then serve as the fracture site. In addition to the bonding fracture, the possibility of carbide formation appears to be supported by the softening of L-605 near the interface. In any event, the present results on the R-41 / Mo-0.5Ti couple demonstrated an additional aspect of diffusion bonding in that the nature and strength characteristics of the bonding interface can be controlled to some extent by one or more intermediate layers.

Couple #2 Cb-1Zr to 316 SS

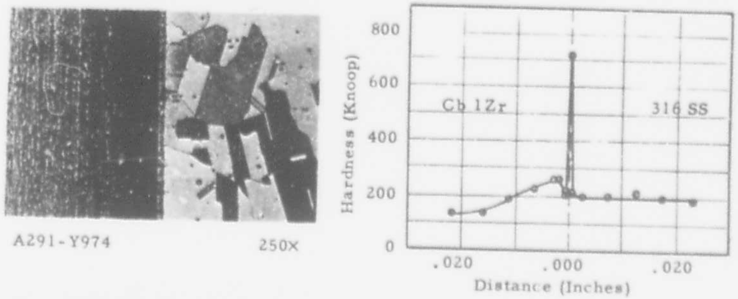

Couple #10 Cu to Cb 1Zr

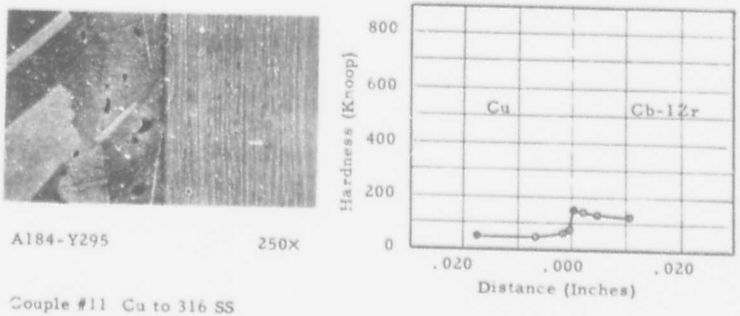

Couple #11 Cu to 316 SS

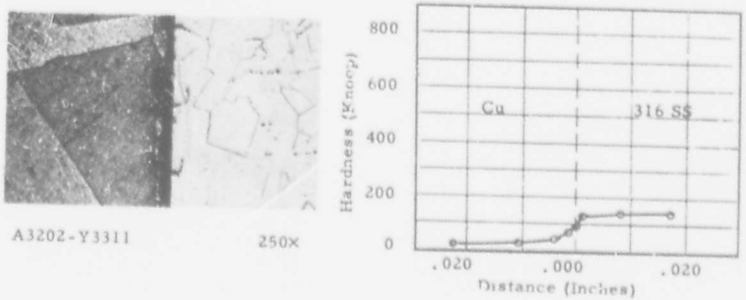

Figure 19. Microstructure And Hardness Characteristics Of Selected Combinations As-Bonded At 1800°F/4 Hours/Vacuum.

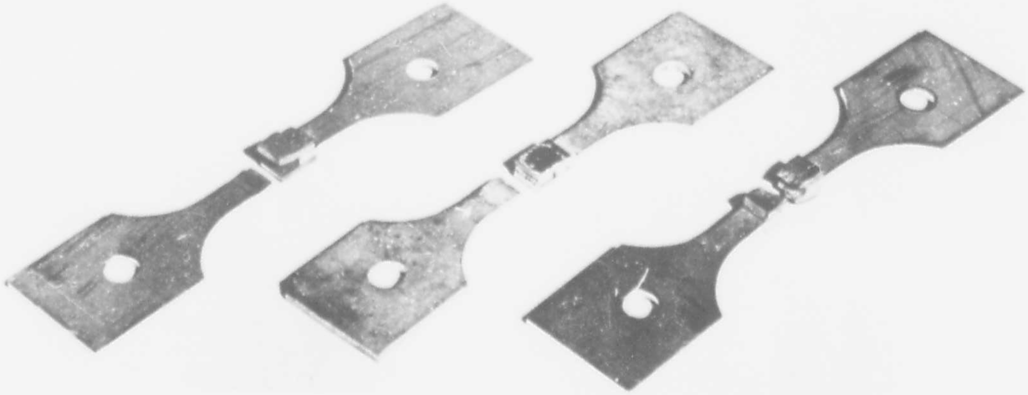

(A) (B) (C)

FIGURE 20. TENSILE SHEAR SPECIMENS TESTED AT ROOM TEMPERATURE.

(A) Cb-1Zr (double laps) to 316 SS - bond shear failure

(B) Cb-1Zr (double laps) to Cu - Cu sheet failure

(C) Cu (double laps) to 316 SS - Cu laps ruptured

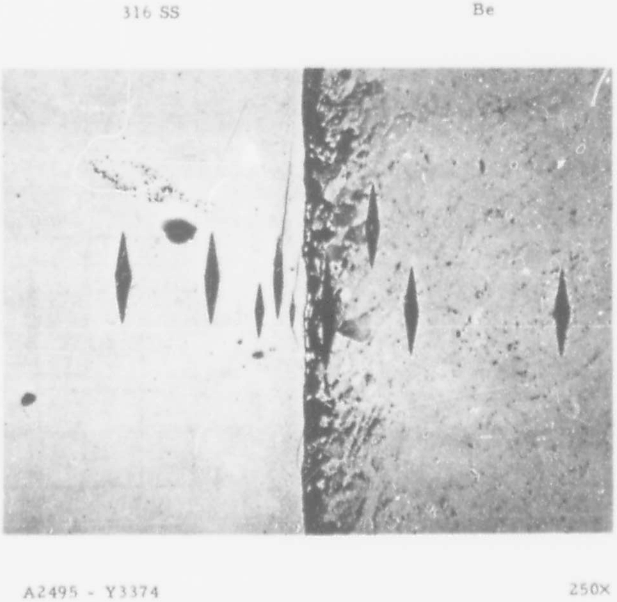

Figure 21 : Microstructure Of 316 SS - Be Couple Bonded At 1800°F/4 Hr. /Vacuum

A. Mo-0.5Ti/R-41 : 2000°F/4 hrs.

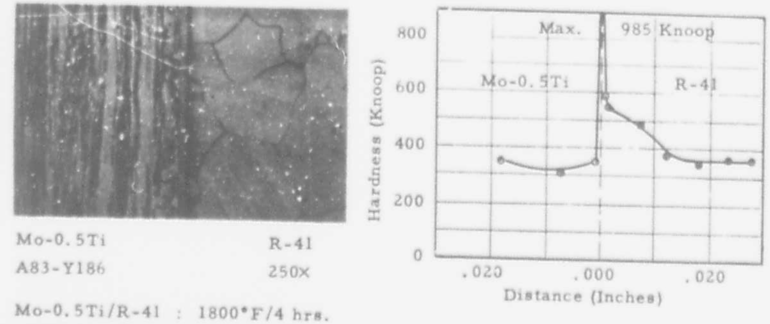

B. Mo-0.5Ti/R-41 : 1800°F/4 hrs.

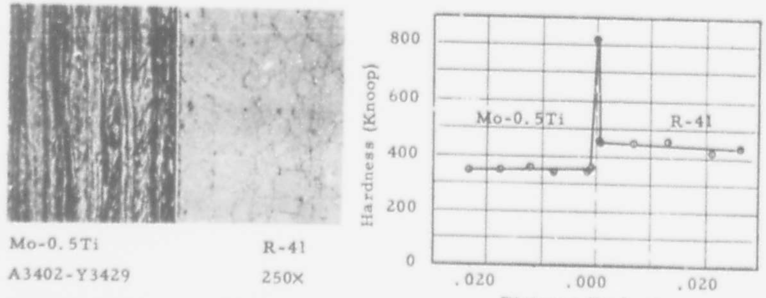

C. Mo-0.5Ti/Cr/R-41 : 1800°F/4 hrs.

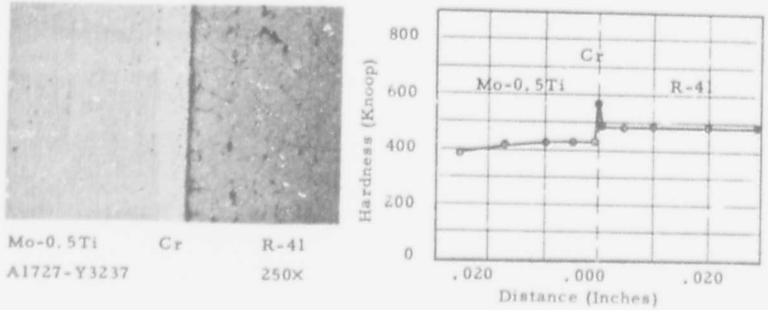

Figure 22 : Microstructures And Hardness Traverses Of Mo-0.5Ti To R-41 With And Without Cr Barrier.

A. Mo-0.5Ti/L-605 : 2000°F/4 hrs.

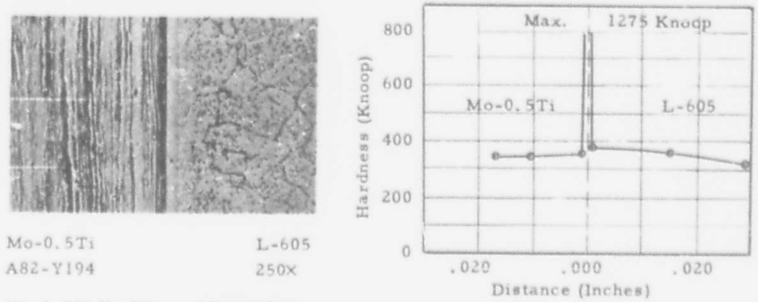

B. Mo-0.5Ti/L-605 : 1800°F/4 hrs.

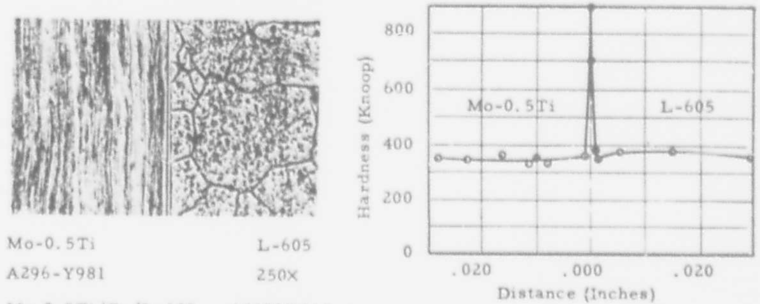

C. Mo-0.5Ti/Cr/L-605 : 1800°F/4 hrs.

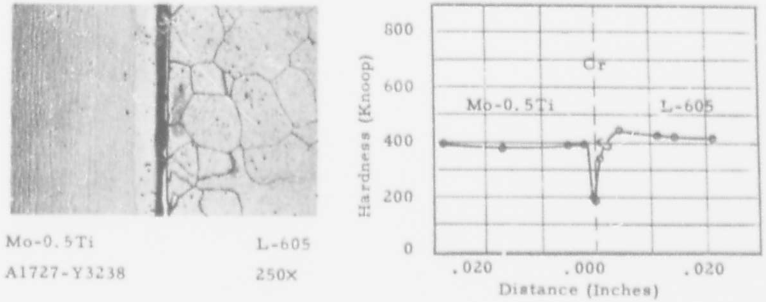

Figure 23 : Microstructures And Hardness Traverses Of Mo-0.5Ti To L-605 With And Without Cr Barrier.

REFERENCES

1. Young, W. R., "Alloy Systems For Brazing Of Columbium And Tungsten", ASD Tech. Report 61-592, January, 1962.

2. Hughes, J. and Geach, G., "The Alloys Of Rhenium With Molybdenum Or With Tungsten And Having Good High Temperature Properties", 1955 Plansee Proceedings, p. 245, Pergamon Press, London, 1956.

3. Clark, J. W., "Physical Metallurgy Of Welding Tungsten And Tungsten-Base Alloys", ASD Tech. Report 61-584, January, 1962.

4. Ratliff, J. L., et al, "Development Of A Ductile Tungsten Sheet Alloy", Battelle Summary Report, May 26, 1962.

5. Young, W. R., Clark, J. W., and Jones, E. S., "Investigation Of The Physical Metallurgy Of Joining Tungsten And Columbium", Air Force Contract #33(616)-7484, Quarterly Progress Reports, February 9 and May 7, 1962.

6. Allen, B. C., Maykuth, D. J., and Jaffee, R. I., "The Effects Of Impurities On The Properties Of Tungsten", AFSW Technical Report 60-6, December, 1959.

7. Rutherford, S. L., Mercer, S. L., and Jepsen, R. L., "On Pumping Mechanisms In Getter-Ion Pumps Employing Cold-Cathode Gas Discharges", 1960 Vacuum Symposium Transactions, Pergamon Press, London, 1961.

8. Hansen, M. and Anderko, K., "Constitution Of Binary Alloys", McGraw-Hill Book Company, Inc., 1958.